Study on Degradation of Solid Oxide Fuel Cell With Pure Ni Anode

Zhenjun Jiao[a], Naoki Shikazono[a] and Nobuhide Kasagie[b]

[a] Institute of Industrial Science, the University of Tokyo, Tokyo, Japan
[b] Department of Mechanical Engineering, The University of Tokyo, Tokyo, Japan

In this study, the degradation phenomena at the interface between Ni and YSZ have been investigated by using screen-printed pure Ni anode sintered on YSZ pellet. The time depended microstructural evolution of Ni-YSZ interface in long time galvanostatic polarization is studied in hydrogen with different humidity. The microstructural changes were characterized by scanning electron microscopy (SEM). Influence of bulk gas humidity, silica impurity aggregation and Ni redistribution at TPB were investigated. The degradation mechanism at Ni-YSZ interface is discussed.

Introduction

Solid oxide fuel cell (SOFC) has attracted more and more attentions in the last few decades as an attractive device. SOFC has the advantages such as fuel flexibility and high efficiency (1). The current challenge focuses on the long-time stability and durability of SOFC electrode. In the industrial applications, a durability of more than 40,000 hours is expected, while current SOFC anodes always exhibit significant degradation in long time discharging experiments, which is often caused by the coarsening of Ni (2,3). With higher current density or overpotential, rapid degradation or even sudden failing of the cell can be observed (4).

Experimental

NiO powder used in this study has an average particle diameter of 1.1 µm. The powder was mixed with terpineol solvent and the ethylcellulose binder in agate mortar to obtain anode screen-printing slurry. The slurry was screen-printed onto commercial dense YSZ pellet (diameter 20 mm, thickness 0.5 mm) with a diameter of 10 mm and then sintered at $1400^{o}C$ for 3 hours to obtain a strong bonding between YSZ and NiO.

$(La_{0.8}Sr_{0.2})_{0.97}MnO_3$ (LSM) powder (0.4 µm) mixed by YSZ powder (0.1 µm) in a mass ratio of 1:1 was used as cathode material. The powder was mixed with the terpineol solvent and the ethylcellulose binder in agate mortar to obtain cathode printing slurry. The slurry was screen-printed onto the counter side of the commercial YSZ pellet with a diameter of 10 mm as cathode. The cathode was sintered at $1200^{o}C$ for 3 hours.

The details of SOFC performance measurement setup have been introduced in the previous paper (5). The YSZ pellet was surrounded by a Pt wire as reference electrode. Pt paste was used to enhance the conductive connection between Pt wire and YSZ pellet. Nitrogen was used as the protective gas in the initial heating up stage. After the furnace temperature had been increased to $700^{o}C$, glass seals completely melt over the edges of

the cell, the reference electrode and two outer tube edges, which resulted in good sealing. Then, dry hydrogen gas was introduced to reduce the porous NiO pellet for 1 hour before cell testing was conducted. The performance of SOFC was evaluated at 800°C by using humidified hydrogen as a fuel and pure oxygen as an oxidant. Anode-reference static current method, with a current density of 200 mA/cm^2, was applied to test anode durability within hydrogen humidified by different concentration of humidity. After discharge experiment, the cell was rapidly cooled down to room temperature in nitrogen the gas.

Observation of the sample microstructures was facilitated by FIB-SEM (Carl Zeiss, NVision40). The secondary electron images of YSZ surface were obtained by chamber detector and Ni surface by in-lens detector. The elements analysis was accomplished by energy dispersive X-ray spectroscopy (EDX; Thermo Electron, NSS300).

Results and Discussions

Experimental Results

The anode-to-reference discharge test was conducted in four humidity conditions: dry, 3% H_2O, 10% H_2O and 30% H_2O. Figure 1 shows the transient performances of the four cells with a discharge time of 100 hours. It can be seen that the all the performances of anodes within dry, 3% H_2O and 10% H_2O hydrogen conditions present different degradation rates through 100 hours from the beginning of discharge. The degradation rates in dry hydrogen and 30% H_2O hydrogen are larger than in 3% H_2O hydrogen and 10% H_2O hydrogen cases. For the cell tested in dry hydrogen, the anode degradation rate decreases with time and the performance tends to be stable after about 60 hours. For the cell tested in 30% H_2O hydrogen, there is a sudden failing of the anode before reaching 20 hours discharge. Cells tested in 3% H_2O hydrogen and 10% H_2O hydrogen present a relative stable state from the beginning of the discharge and stage lasting time increases with humidity. After the initial stable stage, a relatively slower degradation followed for both cases. In addition, the performances of the cells tested in high humidity hydrogen (10% H_2O, 30% H_2O) show some irregular pulse signals, comparing to the smooth degradation process within low humidity hydrogen (dry, 3% H_2O).

Microstructure

Figure 2 shows the top views of anodes after reduction and after discharge within different humilities. From the comparison, it is clearly seen that after discharge, anode was partially delaminated from electrolyte surface and no delamination can be observed after reduction. With the increase of humidity, more Ni was delaminated. Besides, the YSZ surface around anode become black after operating in dry hydrogen.

Figure 3 shows YSZ-NiO interface after sintering and the YSZ-Ni interface after reduction. Bonding strength between YSZ and NiO has been proved to be stronger than that between YSZ and Ni (6). In high temperature sintering (around 1673 K), molten Ni-oxygen eutectic mixture can be formed so that the stress caused by the thermal mismatch between NiO and YSZ can be relaxed due to the YSZ surface pattern formed in sintering and the presence of liquid phase. Upon solidification of the eutectic melt, a strong bond

can be established. After reduction, a clear boundary can be observed between Ni and YSZ phases, while nano-size pores can also be observed which is caused by the reduction of Ni phase.
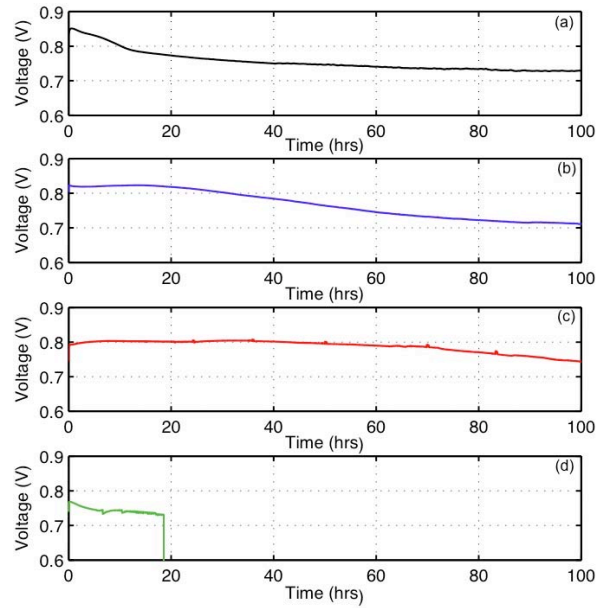
Figure 1. Anode-to-reference terminal voltage within (a) dry, (b) 3% H_2O, (c) 10% H_2O and (d) 30% H_2O hydrogen with a discharge current density of 200 mA/cm^2.
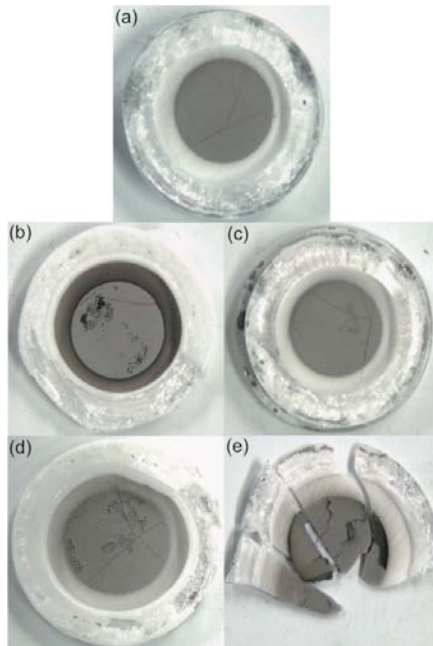
Figure 2. Top views of the anodes. (a) Just after reduction, (b)-(e) after discharge corresponding to Figure 1 (a)-(d).
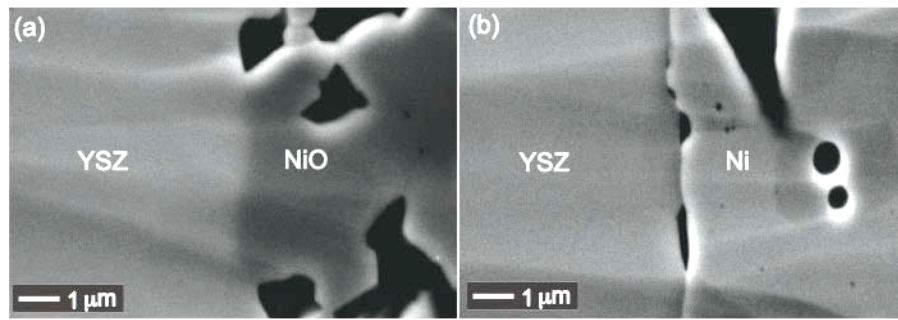
Figure 3. (a) YSZ-NiO interface after sintering. (b) YSZ-Ni interface after reduction.
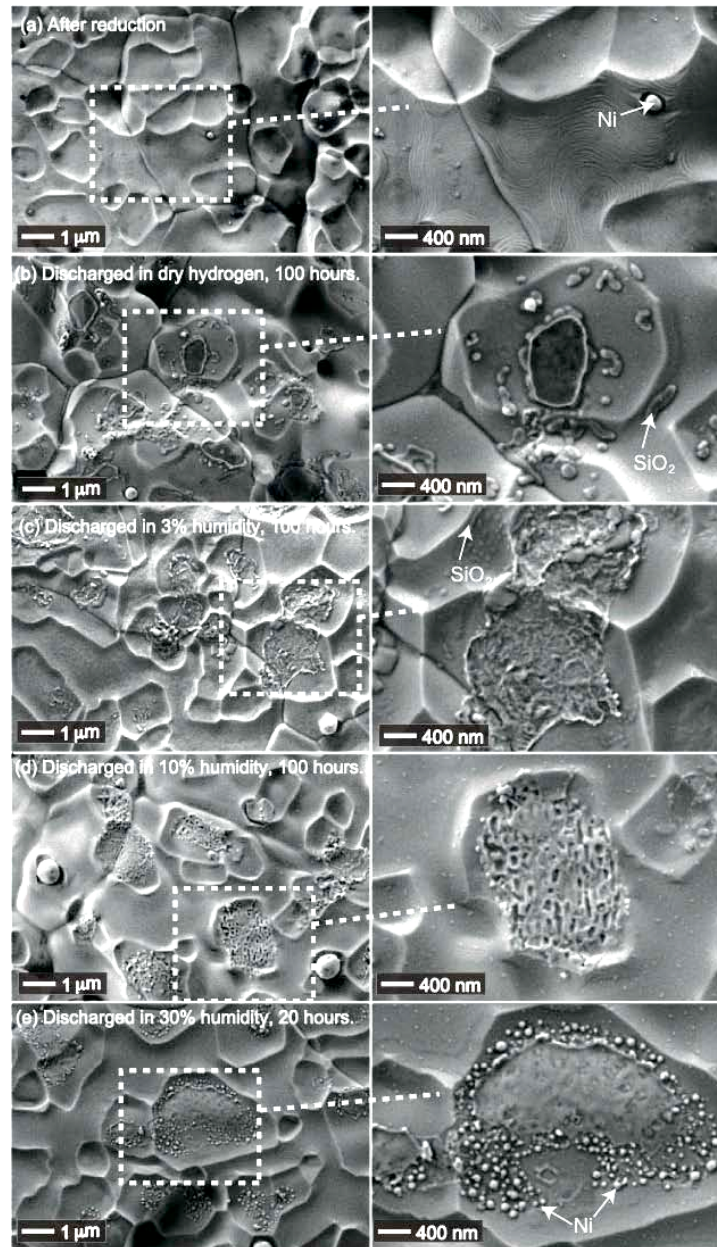
Figure 4. Top views of YSZ-Ni interfaces (a) After reduction, (b)-(e) after discharge corresponding to Figure 1. (With Ni anode mechanically stripped off from YSZ surface.)

Figure 4 shows the YSZ-Ni interface after reduction and discharge within different humidified hydrogen environments. Ni phase has been striped off mechanically after the cell was cooled down to room temperature. After reduction, on YSZ surface, only the pattern formed during the high temperature sintering can be observed, and YSZ surface remained smooth. Certain independent Ni particles were bonded to YSZ surface with a round shape. After discharge, a clear interlayer can be observed at the YSZ pattern bottom. When anode was discharged in dry hydrogen for 100 hours, a smooth interlayer was formed between Ni and YSZ with a clear rim-ridge. With the increase of the humidity in discharging, the interlayer become rougher and the rim-ridge disappeared. In 30% H_2O, anode failed before 20 hours operation, while interface was smoother than 10% H_2O case. Large amount of independent satellite droplets were observed around the interlayer in dry case and the amount decreased with the increase of humidity, while no obvious droplets can be observed in 10% H_2O case. In 30% H_2O case, another kind of droplet was observed around the interlayer with different morphology. Because of the small size, point EDX method was used to indentify the content of the interlayer and the independent droplets. The main content of the interlayer was found to be an impurity layer composed by a main content of Si compound. The independent droplets in dry, 3% H_2O and 10% H_2O cases were found to be the same Si compound. The droplets in 30% H_2O case were identified to be Ni.

Discussions

Glass ring used in our experiment is made of about 75% SiO_2. SiO_2 can be corroded by reduction with hydrogen at high temperatures and produces gaseous SiO as shown in the following reaction (7):

$$SiO_{2(s)}+H_2 \rightleftharpoons SiO_{(g)}+H_2O \tag{1}$$
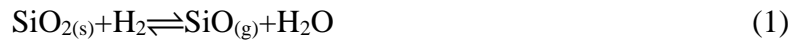
At the same time, Ni phase can be transferred away via volatile $Ni(OH)_2$ from TPB to bulk gas by $Ni(OH)_2$ as shown in reaction (2), which has been reported in Ref. (5).

$$Ni(OH)_{2(g)}+H_2 \rightleftharpoons Ni_{(s)}+2H_2O \tag{2}$$

The partial pressure of different gaseous phase in hydrogen versus humidity was calculated by chemical thermodynamics software FACT and plotted in Figure 5. With the increase of humidit, the partial pressure of gaseous SiO decreases while the partial pressure of gaseous $Ni(OH)_2$ increase. The local concentration at TPB can be much higher than bulk gas in the process of discharging (5). The gradient of humidity from bulk gas to local TPB can drive the transfer of gaseous SiO from bulk gas to TPB where the reaction (1) was driven to left hand side and stable SiO_2 was produced and accumulated at TPB to form a clear rim-ridge. At high temperature the liquid phase glass phase formed by SiO_2 and the other impurities can penetrate into the gap between Ni and YSZ formed in reduction as shown in Figure 3. The interlayer can partially block the active TPB and cause the fast degradation of anode. Because of the relatively high concentration of SiO in the bulk gas, some deposition happened around TPB region and formed the independent glass droplets away from TPB.
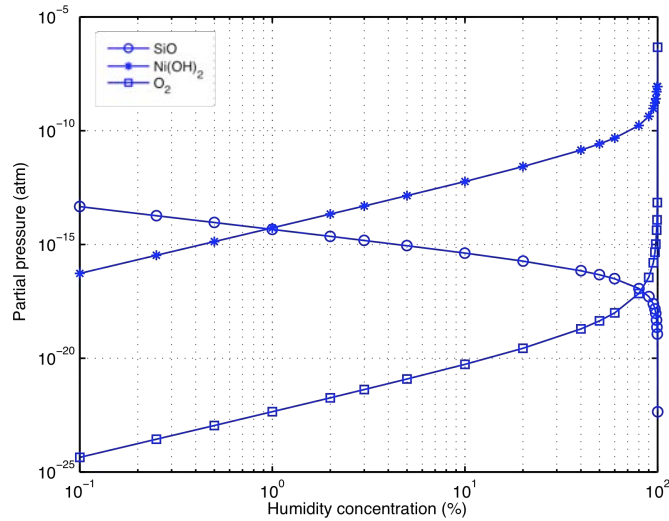
Figure 5. Partial pressure of gaseous phases versus humidity in hydrogen.

With the increase of humidity, the lower SiO gaseous concentration in bulk gas prohibits accumulation and penetration. In high humidity, the surface diffusion of Ni can be accelerated to hundred times faster than in dry hydrogen (8). The aggregation of Ni particle can rapidly change the Ni-YSZ boundary where active TPB located. With the total current density kept constant, the local current density increased with time and further enhanced the degradation, which led to the lose of Ni-YSZ bonding and the delamination of Ni from YSZ surface. Because of the fast bonding lose, the formation of accumulated SiO_2 rim-ridge was prohibited. Instead, a rough surface of glass interlayer was formed by the aggregation of SiO_2. With less accumulation of glass phase, a relative small degradation rate was observed in anode discharge tests. When the humidity was very high, like 30% H_2O case, very fast aggregation of bulk Ni phase can cause fast degradation of Ni-YSZ interface by reducing the active TPB density, and led to sudden failing. At the same time, the lower humidity gradient leads to a local deposition of Ni droplets as shown in Figure 4 (5).

The accumulation of SiO_2 and the change of Ni phase morphology together determine the cell performance and the Ni-YSZ interface change. The mechanism is illustrated in Figure 6. When SiO gaseous phase was cooled rapidly, it condenses to form a glassy brown/black amorphous solid, which oxidize in air giving SiO_2. This property explains the black coating phenomena on free YSZ surface in dry hydrogen, and the YSZ surface under anode in the other cases as shown in Figure 2 (b). The silicon content impurity may be not just caused by the segregation of materials impurity in discharging process but also the deposition of gaseous SiO in bulk hydrogen caused by reaction (1). At the same time, with the presence of ZrO_2, Zirconium Silicate ($ZrSiO_4$) can be produced in a reaction (10,11) in hydrogen reduction environment, and change the surface morphology of YSZ according to Figure 4.

$$SiO_{2(s)}+ZrO_{2(s)} \xrightarrow[\text{mineralizer}]{\text{humidity}} ZrSiO_{4(s)} \tag{3}$$
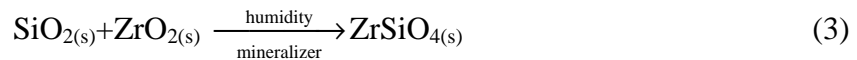
The existing Y_2O_3 and the other impurities were reacted as mineralizer (material which catalyzes the reaction) in reaction (3). The produced $ZrSiO_4$ with pigment can also

explain the dark color film produced in dry hydrogen case, at the same time. The produced SiO_2 can be stabilized by reaction (3). Liu et al. (9) have reported the similar phenomena of the accumulation of glass phase which degrades the anode-electrolyte interface and Ni-YSZ grain boundaries by forming nanometer-thin silicate glass films after long-term discharging testing. The amount, morphology and distribution of the silicate glass were thought to be caused by the segregation of material impurities. Glass is a popular material used for gas sealing in SOFC experiment. In the present experiment, it is considered that glass seal is the main source of silicon dioxide. Further investigation will be carried out in the following study.

Conclusions

Pure Ni anode was used to study the degradation phenomena at the interface between Ni and YSZ. The accumulation of SiO_2 caused by the deposition of volatile SiO was observed. With the morphological change of Ni phase, the degradation of anode was explained. Glass seal ring was suggested to be the main source of silicon. With the influence of bulk gas humidity, the competition between two mechanisms determines the anode performance.

Acknowledgments
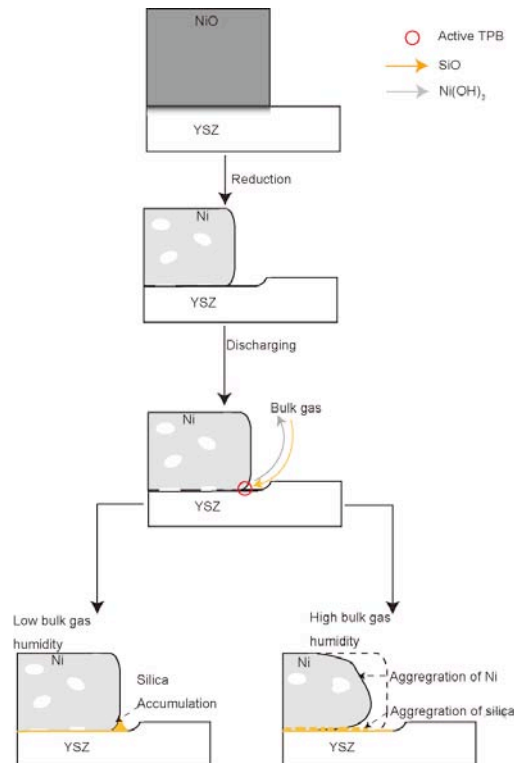
Figure 6. Ni-YSZ interface change mechanism illustration.

References

1. S. C. Singhal, K. Kendall, High Temperature Solid Oxide Fuel Cells: Fundamentals, Design and Applications, *Elsevier Advanced Technology*, (2003).
2. S. Koch, P. V. Hendriksen, M. Mogensen, Y. L. Liu, N. Dekker, B. Rietveld, B. D. Haart, F. Tietz, *Fuel Cells,* 2, 130–136 (2006).
3. S. P. S. Badwal, M. J. Bannister, R. H. J. Hannink, Science and Technology of Zirconia V, Technomic publishing Company, (1993).
4. T. Matsui, R. Kishida, J. young Kim, H. Muroyama, K. Eguchi, J. Electrochem. Soc. 157, B776–B781 (2010).
5. Z. Jiao, N. Takagi, N. Shikazono, N. Kasagi, *J. Pow. Sources*, 196, 1019-1029 (2010)
6. T. Yamane, Y. Minamino, K. Hirao and H. Ohnishi, *Journal of Materials Science*, 21, 4227 (1986).
7. A. F. Holleman, E. Wiberg, *Inorganic Chemistry*, San Diego: Academic Press, ISBN 0-12-352651-5 (2001).
8. J. Sehested, J. A. Gelten, S. Helveg, *Applied Catalysis A: General,* 309 (2), 237 – 246 (2006).
9. Y. Liu, C. Jiao, *Solid State Ionics*, 176, 435 – 442 (2005).
10. P.H. Larsen, "Sealing materials for solid oxide fuel cells", *PhD thesis*, Sheffield University, UK, 1999.
11. E. Garcia, J. M. Guimaraes., P. Miranzo, M. Osendi, C. Co jocaru, Y. Wang, C. Moreau and R. Lima, *Journal of Thermal Spray Technology* 20 (1), 83–91 (2011).